

Image-Based BRDF Measurement*

Stephen R. Marschner
Eric P. F. Lafortune
Stephen H. Westin
Kenneth E. Torrance
Donald P. Greenberg

PCG-99-1

January, 1999

We present a new image-based process for measuring surface reflectance rapidly, completely, and accurately. Requiring only a digital camera, a light source, and a convex curved test sample, our method can measure the BRDF with high resolution and accuracy over a very large domain of illumination and reflection directions. We have verified our measurements both by tests of internal consistency and by comparison against measurements made using a gonireflectometer.

*This report was submitted for publication at SIGGRAPH 99.

Image-Based BRDF Measurement

Category: research

Abstract

We present a new image-based process for measuring surface reflectance rapidly, completely, and accurately. Requiring only a digital camera, a light source, and a convex curved test sample, our method can measure the BRDF with high resolution and accuracy over a very large domain of illumination and reflection directions. We have verified our measurements both by tests of internal consistency and by comparison against measurements made using a gonioreflectometer.

1 Introduction

The science of rendering images that faithfully represent the true behavior of light has advanced in accuracy and generality at the same time that computation power has become continually more plentiful. For the powerful rendering systems that result from these trends to realize their full potential they must begin with better input than ever before, and a fundamental part of that input is surface reflectance.

Advanced rendering systems have a continuing need for more nuanced reflectance models that not only conform to physical laws and exhibit well-known properties of real surfaces but also model the characteristic behaviors of particular types of material. The development of models that describe real materials inherently depends on the ready availability of good BRDF measurements.

The fundamental description of surface reflectance is the *bidirectional reflectance distribution function* (BRDF), which describes how a surface reflects light for any illumination direction, any viewing direction, and any wavelength. BRDF measurements have traditionally been made with purpose-built devices known as *gonioreflectometers*, and the difficulty of building and using such devices to make accurate measurements is notorious, with even the best instruments disagreeing by wide margins[12]. The complication and expense involved in working with gonioreflectometers, as well as the long measurement times required by conventional instruments, has discouraged the practice of BRDF measurement, leaving the computer graphics community starved for BRDF data. There is a need for simpler, faster, less expensive techniques that can be widely implemented but still make accurate measurements. Gonioreflectometers are also normally limited to measuring flat samples, and techniques for measuring materials that only occur in curved shapes are desirable.

This paper presents a system that measures reflectance quickly, completely, and without special equipment. The method works by taking a series of photographs of a curved object; each image captures light reflected from many differently oriented parts of the surface. By using a curved test sample and an imaging detector, and by using automated photogrammetry to measure the camera position, we eliminate the precise mechanisms needed to position the source and detector in a conventional gonioreflectometer. With the knowledge of the sample shape and the light source position, the photographs can be analyzed to determine the sample's BRDF. Although the apparatus is simple and the measurement rapid, the resulting data are very accurate and can be very complete, covering the full hemisphere almost to grazing angles.

2 BRDF Background

The reflectance of a surface at a point can be completely characterized by the BRDF. It is called *bidirectional* because it is a function of both the illumination and the reflection directions. Each direction, as shown in Figure 1, can be expressed by spherical coordinates: (θ_i, ϕ_i) for the illumination, or incident, direction and (θ_e, ϕ_e) for the reflection, or exitant, direction. The BRDF ρ_{bd} is the ratio of the radiance exiting the surface in a given direction to the incident

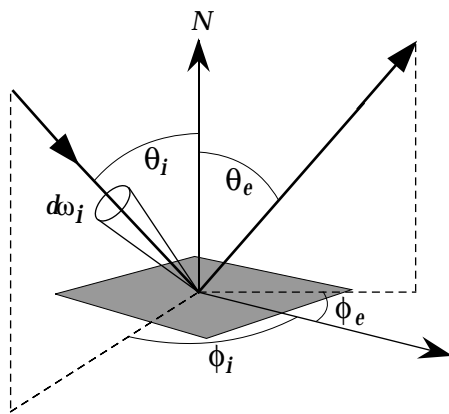


Figure 1: Geometry of Surface Reflection

irradiance of a particular wavelength λ from an incident solid angle $d\omega_i$ about a given illumination direction:

$$\rho_{bd}(\theta_i, \phi_i, \theta_e, \phi_e, \lambda) = \frac{dL(\theta_e, \phi_e)}{dI(\theta_i, \phi_i)}. \quad (1)$$

The BRDF is thus a function of five variables, but its domain is reduced somewhat by a symmetry called *reciprocity*, which states that reversing the light's path does not change the reflectance:

$$\rho_{bd}(\theta_1, \phi_1, \theta_2, \phi_2, \lambda) = \rho_{bd}(\theta_2, \phi_2, \theta_1, \phi_1, \lambda).$$

In this paper we will concentrate on the important class of *isotropic* materials, for which the reflectance is independent of rotating the incident and exitant directions about the surface normal. For these surfaces, the BRDF depends only on $\Delta\phi = \phi_i - \phi_e$, rather than on ϕ_i and ϕ_e , which reduces the domain from five to four variables:

$$\rho_{bd}(\theta_i, \phi_i, \theta_e, \phi_e, \lambda) = \rho_{bd}(\theta_i, \theta_e, \Delta\phi, \lambda). \quad (2)$$

For computer graphics, in which the wavelength dependence of BRDF is of interest only for the purposes of determining colors seen by human observers, the continuous wavelength dimension can be replaced with an appropriate discrete set of three to five measurements, further reducing the isotropic BRDF to a vector-valued function of three variables.

3 Overview of Method

A straightforward device for measuring isotropic BRDFs is shown in Figure 2a, illustrating the three mechanical degrees of freedom required. A flat sample is illuminated by a light source, and a detector measures the complete distribution of reflected light by moving around the entire hemisphere. To measure a full BRDF this process must be repeated many times, moving the light source each time to measure a different incidence angle.

Because the positions of the light source and detector are only relevant relative to the plane of the surface, exactly the same measurements could be made using the device of Figure 2b, in which the sample rotates with two degrees of freedom but the detector has only one and the source is fixed. The number of degrees of freedom remains the same, and all the same configurations of source, sample, and detector can be achieved.

Both of these devices require physical movement for the measurement of every BRDF sample. Because of this, complete measurements will take a long time. If the sample is curved, instead of flat, every part of the sample's surface has a different orientation, and instead of rotating the sample we can simply measure different parts of the surface by using a camera for the detector, as shown in Figure 2c. In this device, the two dimensions of the image sensor substitute for the two degrees of freedom of sample rotation. If there is sufficient curvature, we can make all

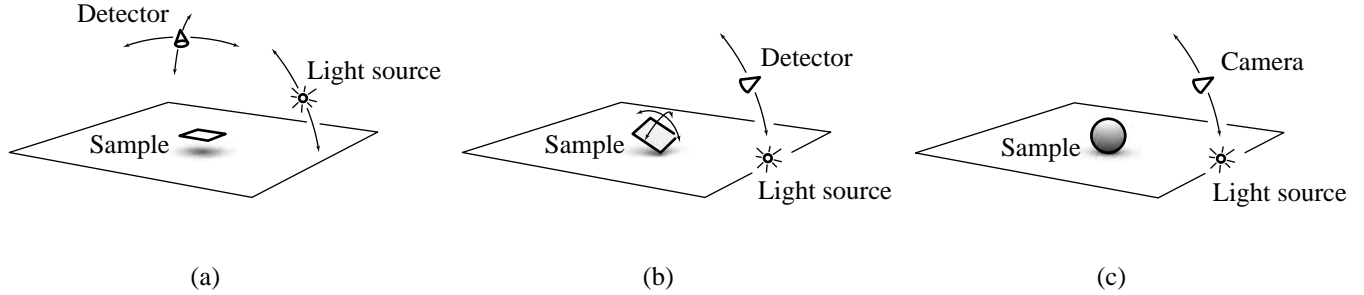


Figure 2: Three BRDF measurement devices, leading to our image-based approach (c).

the same measurements as the other devices, but by measuring two degrees of freedom in parallel we can greatly reduce the measurement time while increasing the sampling density.

This is the essence of image-based BRDF measurement. In an image of a curved object taken using a small light source, every pixel is in effect a BRDF measurement. Given a 3D model of the sample, camera, and light source, we can determine the incident and exitant directions for each pixel relative to the surface normal, as well as the irradiance of the light source. Together with the radiance measured by the camera, these are all the data required to compute the BRDF.

A single image will only cover a two-dimensional subset of the possible BRDF configurations, so many images are required to measure the whole domain. In the case of an isotropic BRDF, we are filling up the three-dimensional domain of the BRDF by measuring two-dimensional sheets, so we will need a one-dimensional sequence of images, with the camera or light source positioned differently in each.

4 Related Work

The BRDF is a function of five variables: two for the illumination direction, two for the reflection direction, and one for wavelength. Many materials are isotropic—they have no grain, or directionality, to the surface—and for these surfaces, as detailed in Section 2, the BRDF has just four degrees of freedom. Sampling this high-dimensional space sequentially is impractical, but measuring multiple points simultaneously can speed data collection.

Traditionally [14, 16], the three or four angular dimensions are handled by specialized mechanisms that position a light source and a detector at various directions from a flat sample of the material to be measured. The final dimension, that of wavelength, is handled either with a broadband spectroradiometer that measures the entire spectrum at once, or by multiple measurements varying the wavelength of a narrow-band source or detector. Because three, four, or five dimensions must be sampled sequentially, measuring reflectance functions can be time-consuming, even with modern computer controls. Moving the motor stages and measuring the reflected light can take several seconds, and since measurements are taken point by point, even a sparse sampling of the incident and exitant hemispheres can take several hours.

More recently, techniques have been reported to speed measurements by gathering many angular samples at once. These methods, including the method presented in this paper, use a two-dimensional detector—the image sensor of a digital camera—to measure a two-dimensional range of angles simultaneously, leaving one or two dimensions of angle and one dimension of wavelength to be sampled by sequential measurements.

These can be categorized in two groups: those that attempt to measure the BRDF over its entire bihemispherical domain, and those that measure some useful subset. The BRDF over a subset of the domain can sometimes be useful to deduce characteristics of the surface microgeometry or to find parameters for a low-dimensional BRDF model.

One example of measuring a subset of the domain is the work of Karner et al. [10], who describe a system using an inexpensive CCD camera and a simple incandescent lamp. In their technique, the camera captures an image of a large flat sample and a flat reference surface, which are illuminated symmetrically by the small light source. The different points on the samples have different illumination and reflection directions; because of the symmetry of illumination, the BRDF values can be computed from the ratios between corresponding pixels on the two samples. They use these data to fit coefficients for a low-dimensional reflection model.

Ikeuchi and Sato [9] present a system for estimating reflectance model parameters using a surface model from a range scanner and a single image from a video camera. They use a curved sample to capture a set of directions spanning a large range of both incidence and exitance angles, within the set of angles provided by the illumination and view angles of a single image.

Sato et al. [15] describe a method to fit BRDF parameters from a sequence of images of an arbitrarily shaped object under controlled illumination. They use the two dimensions of the captured images to capture the spatial variation of BRDF across the surface, rather than to sample angular parameters of a spatially uniform BRDF. The image sequence provides samples along a one-dimensional path for each surface point; a simple reflectance model is fit to these data. By using several images, they extend the domain coverage.

The surface optics literature includes a number of approaches to measure a subdomain of the BRDF rapidly; these are generally used to deduce physical parameters of the surface itself, such as feature size on integrated circuits [8] or surface roughness [1], and often measure only at a single wavelength.

Ward [17] presents a device to measure the complete BRDF of anisotropic materials by using a hemispherical half-silvered mirror to gather light scattered from a flat sample into a CCD camera with a fish-eye lens. The camera thus captures the entire exitant hemisphere at once for each illumination direction, leaving two degrees of freedom to handle mechanically. This provides significant time savings over the four degrees of freedom required by the conventional approach.

The most recent publication in this area is the work of Lu, Koenderink, and Kappers [13] on the BRDF of velvet. They use a cylindrical sample to give broad angular coverage in the incident plane, with multiple images using different source positions to cover all angles.

Like these other image-based systems, the system presented in this paper uses a camera to sample a two-dimensional set of angles in a single measurement, so it shares their advantages in speed and sampling density over traditional approaches. It can be thought of as a combination and extension of the techniques of Ward and Lu et al. By adopting a curved sample, it obviates the fisheye lens and hemispherical mirror of Ward’s method and permits measurements much closer to grazing¹. By using samples of compound curvature, we extend coverage from the incidence plane to the entire BRDF domain. We go beyond both of these techniques in allowing hand-held positioning, obviating any precision source positioning mechanism, and in extending the technique to arbitrary convex objects.

The following sections describe the specifics of our system, give the results of measuring several materials, and demonstrate the accuracy of those results by comparing them to measurements from a gonireflectometer of verified accuracy.

5 Method

Our image-based BRDF measurement technique is capable of measuring two different classes of objects: simple geometric shapes, for which the required 3D model can be defined analytically, and irregular shapes, for which the 3D model is provided by a range scanner.

Geometric shapes, such as spheres and cylinders, can be modeled and aligned very precisely, leading to measurements with low error. Also, this approach requires much less equipment, since a range scanner is not required. However, only certain materials can be measured using these shapes—typically only paints or other man-made coatings that can be applied to any object. In the following sections, we will discuss using either cylindrical or spherical samples.

¹Ward’s device covers angles of up to 45° to 75°, depending on azimuth angle, according to the LBL technical report[7]

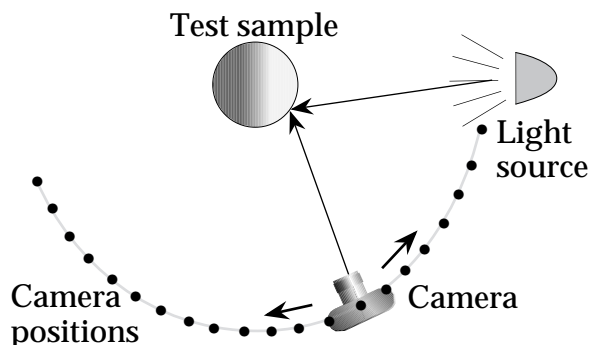


Figure 3: Schematic of Measurement Setup

Using a range scanner to provide the model allows the measurement of any convex object that has a uniform BRDF. Since we no longer have to control the geometry, it becomes possible to measure many more interesting materials. However, range scans are less accurate models, so the error in the data increases somewhat.

5.1 Measurement technique

A session of image-based BRDF measurement begins with setting up the sample. For spherical samples, no additional setup is used; for cylindrical samples a strip of photogrammetric targets is attached to each edge of the sample. For irregular samples, the sample is placed on a platform that contains several photogrammetric targets and the platform and sample are scanned together, so that the surface geometry is measured and simultaneously located in relation to the targets.

Once the sample is ready, it is placed near a reference structure covered with photogrammetric targets that will be used to locate the camera. We then use a hand-held camera to photograph the sample from a sequence of positions, with a single stationary light source providing the only illumination. The camera positions range from next to the light source, which allows measurement of near-retroreflection, to opposite the light source, where we measure grazing-angle reflection (Figure 3). A few additional photographs, described below, are also taken to measure the location and intensity of the light source. In all, a typical measurement session, including the range scan and all the photographs, takes about half an hour.

The equipment we use to make our measurements includes:

- A 1.5 megapixel CCD still camera with an RGB color filter array (Kodak DCS 420).
- A simple industrial electronic flash.
- A structured-light range scanner, for measurements of irregularly-shaped samples (Cyberware 3030/PS).

5.2 Sampling Pattern and Coverage

As explained in Section 3, each image can measure at most a two-dimensional set of BRDF configurations. From each pixel in each measurement image we derive one sample somewhere in the domain of the BRDF; the locations of the samples are determined by the geometry of the sample's surface and the arrangement of camera, source, and sample.

To clarify the sampling coverage, consider the simple case of measuring a cylinder. Since the cylinder's curvature lies along a single direction, we can arrange for the light source, camera, and surface normal always to lie in a plane. Each image will give a set of samples in the incidence plane, with a range of values for θ_i and θ_e . As we move the camera from near the source to opposite the source, this set of (θ_i, θ_e) pairs changes as illustrated in Figure 4. A full set of such images fills up the half of the (θ_i, θ_e) square for which $\theta_i < \theta_e$ (since the camera is to the left of the light source). The principle of reciprocity automatically fills in the other half; in fact, with the assumption of isotropy

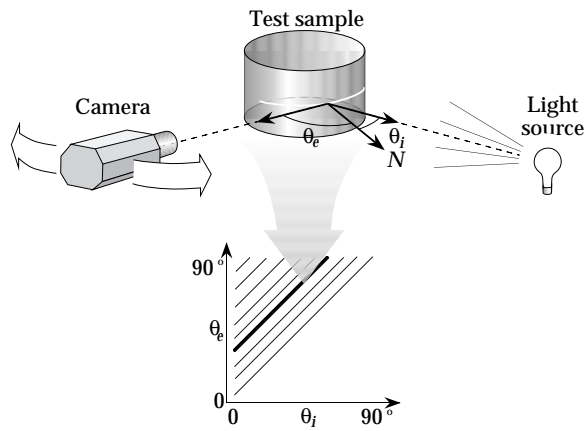


Figure 4: Incidence plane coverage for measurements of a cylinder.

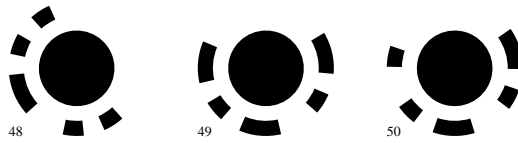


Figure 5: Photogrammetric targets

there is a second symmetry, so we have redundant data that can be compared to verify the measurement or averaged to reduce noise.

If we use a sample with compound curvature, we can measure more than just a single plane. In this case, each image fills a 2D subset of the 3D BRDF domain, and just as with the cylinder it is possible to fill enough of the BRDF domain that reciprocity will fill the rest. With isotropy and bilateral symmetry there is again redundancy that can be used to check the results or to reduce noise.

5.3 Calibration

Turning the camera images into accurate BRDF measurements requires both geometric and radiometric calibration. Geometric calibration establishes the relative positions of the light source, sample, and camera for each measurement image, and radiometric calibration determines the irradiance from the source and the relationship between pixel values and radiance reflected from the sample.

5.3.1 Geometric calibration

The geometric calibration is done with photogrammetric techniques, using machine-readable targets that are placed on a special structure near the sample. The images of these targets are located and identified automatically in each image using ID codes embedded in the targets (Figure 5). The information that must be derived from the target locations includes:

- The position of the light source.
- The camera pose for each measurement image.
- The pose of the sample.

The poses of the cameras are found, using bundle adjustment² [2, 5], from the image-plane target locations. The light source position is found by including a few extra photographs that contain images of targets attached to the light source. The pose of the sample is found using targets attached to the sample, which are also imaged by the range scanner for scanned samples³.

5.3.2 Radiometric calibration

In order to make BRDF measurements for each pixel, we must know the radiance reflected to the camera and the irradiance due to the source. To use a CCD camera to measure radiance requires characterizing both the radiance transfer function, which relates the digital count reported for a pixel with the image-plane exposure, and the flat-field response, which relates the image-plane exposure to radiance in the scene. We measured and corrected for both of these camera characteristics; the details of the procedures are beyond the scope of this paper.

We determined the irradiance due to the source from its measured position and the location of the surface point being measured by using a point-source model. In order for this model to be valid, the source must be small compared to the distance to the sample, and its angular intensity distribution must be uniform. We measured the angular distribution of the source and verified that, with an additional diffuser, it is sufficiently uniform over the range of angles we use. To get the absolute scale of the BRDF correct, we measured the intensity of the light source relative to the camera's three color sensitivities by photographing a diffuse white reference sample (a Labsphere Spectralon target) in a known position.

5.4 Data processing

Processing the measurement images to extract BRDF samples involves two steps. First, the photogrammetric targets are used to determine the geometric arrangement of the sample, camera, source, and reference white target. Second, all this information is given to a *derenderer*, which computes the BRDF values.

The first step in determining the measurement geometry is to process all the measurement images, together with a few calibration images that include images of targets attached to the source and to the reference white sample, with an automatic target finder that locates all the targets and identifies them by their embedded ID codes. These target locations are then used to solve a bundle adjustment system, which computes the poses of all the cameras and the 3D locations of all the targets. If a range scan is providing the surface model for the sample, the targets attached to the sample are also located in the scan, and a transformation is found to align these scanned targets with the corresponding targets in the bundle adjustment system. This transformation serves to locate the scan of the sample relative to the cameras and light source. If the sample is a sphere to be located without targets, the user specifies points on the boundary of the sample in 3 or 4 images, and a tangent sphere is fit to the corresponding rays to define the sample model. For a cylindrical sample, a cylinder is fit to the 3D locations of the targets attached to the sample's surface.

The *derenderer* is derived from a ray-tracing renderer, and its input is a standard scene description including the cameras, the light source, and a model of the sample. It uses standard rendering techniques [6] to find the intersection point of each pixel's viewing ray with the sample surface and to compute the irradiance due to the source. Rather than using a BRDF value to compute the radiance reflected to the pixel, as a renderer would, the *derenderer* instead divides the pixel's measured radiance by the irradiance of the source to obtain the BRDF value. The *derenderer*'s output is a list of BRDF samples, each including the incident direction, the exitant direction, and the BRDF for that configuration. Separate sample sets are generated from the camera's red, green, and blue pixels.

If a range scan is providing the model of the sample, the points from the scanner are tessellated to define the surface for ray intersection. However, the normal that is used to compute the BRDF sample is derived by fitting a plane locally to the surface, to reduce the effects of scanner noise.

²Bundle adjustment takes the image-plane projections of a set of points in a number of cameras and computes the 3D locations of all the points and the poses of all the cameras by solving a nonlinear system of equations.

³When we are using a spherical sample and wish to avoid occluding any part of the surface with targets, a set of points on the silhouette of the sphere is identified by hand in each of a few images and a tangent sphere is fit to the corresponding rays.

To produce a smooth, continuous function from the arbitrarily arranged BRDF samples, we use local polynomial regression in the 3D BRDF domain [3]. Local polynomial modeling involves a kernel that is used to select points near where the reconstructed function is to be evaluated; because our method produces samples densely packed on 2D sheets that are loosely packed in the 3D domain, we use an elliptical kernel to span the distance between the sheets without blurring more than necessary along the sheets. Local quadratic regression was used to produce the reconstructed BRDFs shown in the results.

6 Results

We have used our image-based system to measure the BRDFs of many materials. Two samples representative of the range of possible measurements are a gray painted cylinder, which gives data in the incidence plane only for a controlled artificial coating, and a squash, which is an irregularly shaped natural object with a complex surface material.

For the cylinder measurement, we compared our results against measurements of a matching sample by a calibrated gonireflectometer (measurements courtesy of the Cornell Program of Computer Graphics [4]).

6.1 Gray cylinder

To verify the correctness of our measurements, and to demonstrate the accuracy that is possible under controlled conditions, we painted a section of aluminum tubing (outside diameter 6 inches) with a gray spray-paint primer. The resulting sample has quite uniform surface and is well modeled by an ideal cylinder. We located the cylinder using a strip of photogrammetric targets along each edge; a typical measurement image is shown in Figure 6. Because a cylinder curves only along one direction, the resulting data lie very near a two-dimensional slice of the three-dimensional (isotropic) BRDF domain; the cylinder allows us to concentrate our precision on the incidence plane, where many features of BRDFs are found.

Figure 7 summarizes the results of the gray cylinder measurement (similar summaries will be shown for all the measurements reported). Each row corresponds to a single fixed angle θ , with $\theta = 0$ at the top and $\theta = 75^\circ$ at the bottom. The left column illustrates the sampling pattern in the BRDF domain. Blue points plot the exitant directions of samples with incident directions very close to $(\theta, 0)$ and red points plot the incident directions of samples with exitant directions very close to $(\theta, 0)$ ⁴ Even though θ acts as both incident and exitant angles, we will often call it the incident angle for the sake of brevity. We plot data close to the desired angle because, since we do not directly control the sampling pattern, we cannot in general expect to find samples with θ_i or θ_e exactly equal to θ . However, the density of our data is such that we obtain the large numbers of samples shown in the plots with a threshold of a small fraction of a degree.

In the case of the cylinder, these coverage plots show that the data cover only the incidence plane, as expected. For $\theta = 0$ they cover the whole hemisphere because for normal incidence all exitant directions are in the incidence plane; in the coverage plots for $\theta = 0$ the angular position of samples is simply a matter of convention. There are never any data within a small circle around the incident direction because there is a limit to how closely the camera can approach the source without colliding physically.

In each summary figure, the second column shows the data that fall near the incidence plane (for the cylinder this includes the majority of the data), along with a slice of the 3D BRDF defined by local polynomial regression on the raw samples. Note that the curve is not a fit only to the points that are plotted with it; rather it is a slice of a 3D function fit to all the data points. Because the curve accounts for more points than are shown, it may sometimes appear to disagree with the points.

In the gray cylinder data (Figure 7), note the low noise and broad coverage—the results are good out to at least 80° . Also note that the red and blue points agree; this demonstrates that our measurements exhibit reciprocity, as

⁴Recall that we are assuming isotropy, so that any configuration with θ_i or θ_e near θ is included in this diagram, rotated to move the corresponding ϕ to zero.

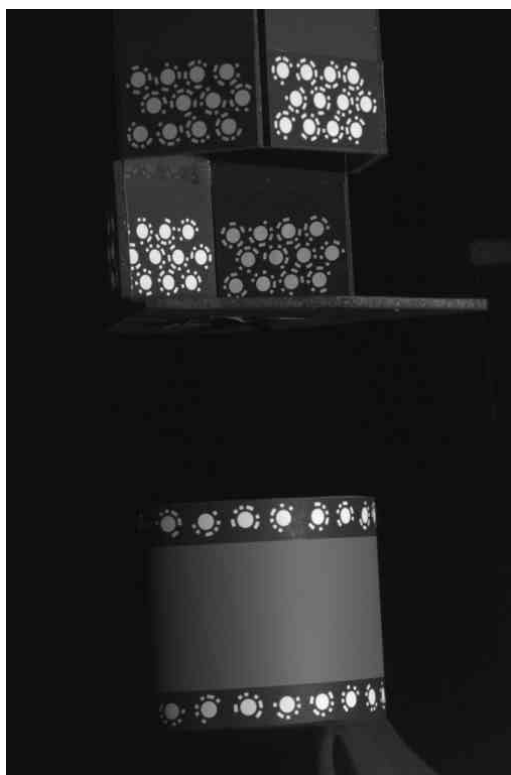


Figure 6: A typical measurement image from the gray cylinder dataset.

must any real BRDF. The red points become noisier near the ends, because these points have near-grazing incidence angles, leading to very low levels of light to be measured and therefore to greater relative noise.

In the gray cylinder measurements only, the third column compares the reconstructed BRDF against independent measurements of a separate, flat, sample painted at the same time as the cylinder. Note the good correspondence; this independent measurement validates the correctness of our method.

6.2 Squash

A much more challenging object serves as the second example: a squash, pictured in Figure 8. This natural object has an irregular yet mainly convex shape, and since it cannot be made into a flat surface without damaging it so as to alter its reflectance, it cannot be measured by conventional means.

A typical measurement image is shown in Figure 8. The support structure containing the photogrammetric targets used to align the range scan with the cameras and light source can be seen below the squash; additional targets for camera pose can be seen above it.

Because of the squash's compound curvature, much of the BRDF domain is sampled, as can be seen from the first column of Figure 9. However, because parts of the surface are obscured there are some gaps in the coverage. The reconstructed curves in the incidence-plane plots (second column) show that the dataset as a whole defines a smooth function that describes an interesting and plausible BRDF, including an off-specular forward scattering lobe and a slow trend toward decreasing BRDF in the backward direction. This is despite the fact that the data contain considerably more noise than do the gray cylinder data. The higher noise is to be expected, given the irregular and non-uniform nature of the surface; the only way to define a single BRDF for an object like this one is to average over the variations.

In this figure, as with the rest of the summary figures, contained in the Appendix, the rightmost column compares the measurements from the three color channels of the camera. In the case of the squash, the approximately constant vertical offset between the curves indicates a near diffuse color, in this case light brown.

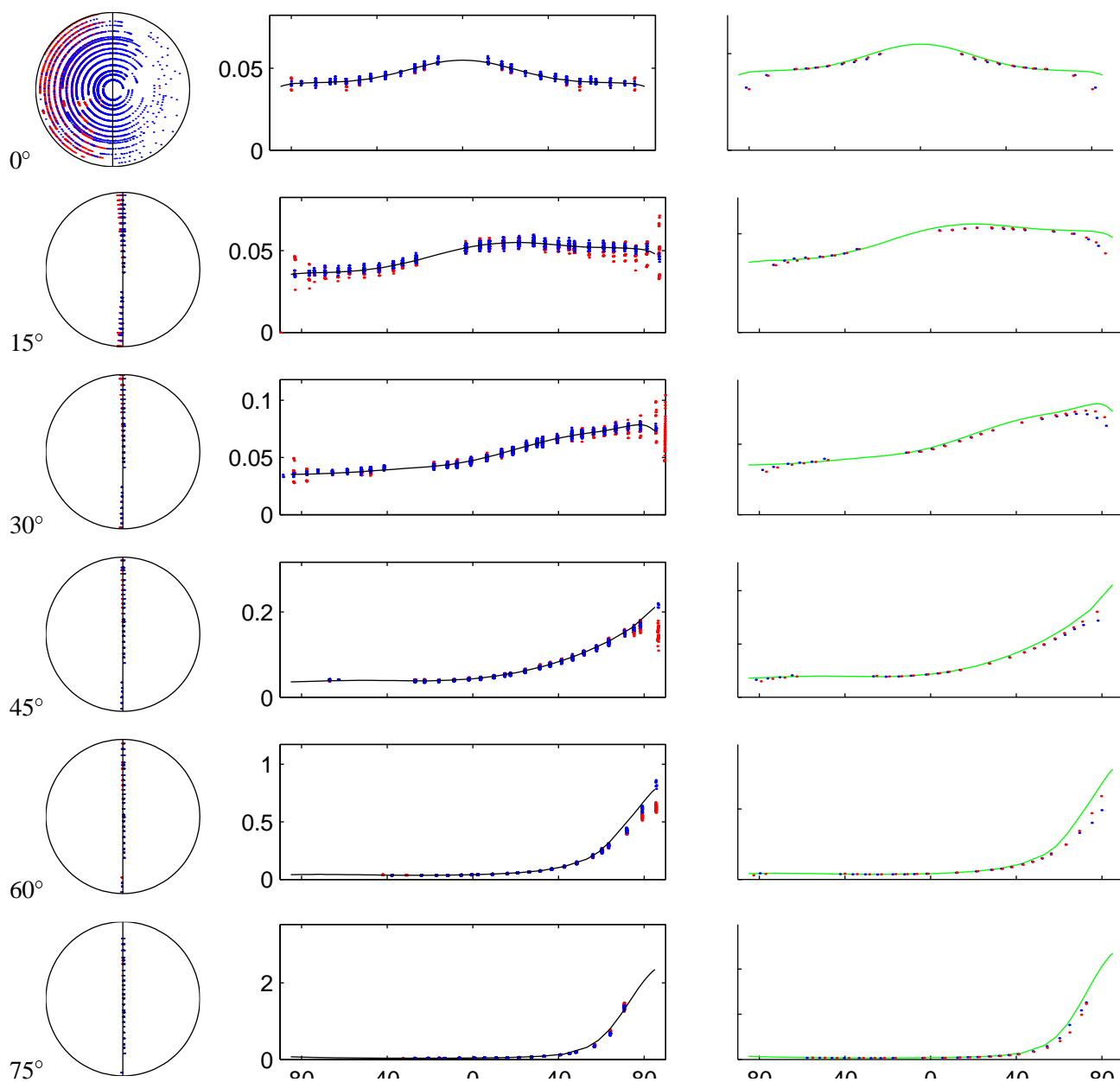


Figure 7: Summary of results for the gray cylinder dataset. Left column: sample coverage; middle column: incidence plane reciprocity and reconstruction; right column: gonioreflectometer comparison. Red points are fixed-incidence samples and blue are fixed-exitance.

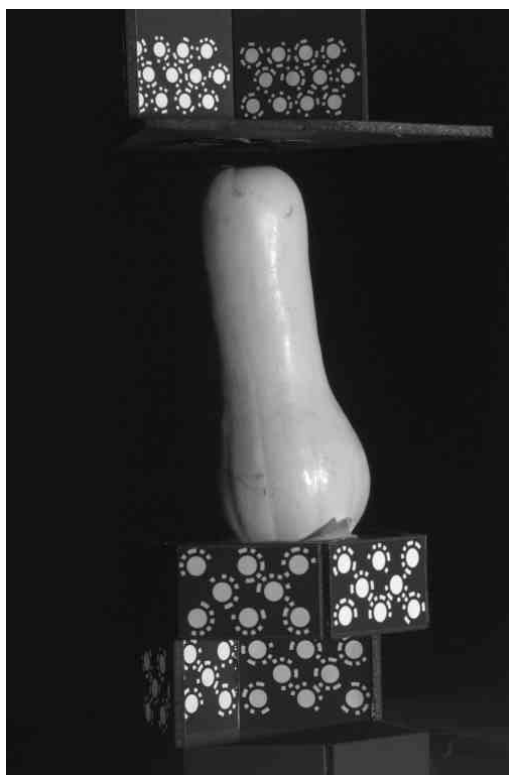


Figure 8: A typical measurement image from the squash dataset.

The summaries for four other samples are given in the Appendix.

6.3 Renderings

Figure 10 shows some visual results of our reflectance measurements. The measurements were approximated with the representation presented by Lafortune et al. [11]. Although the original data have a richer information content, the model captures their main features. Of course other models with more degrees of freedom could be used. The scene is rendered with path tracing. It is illuminated by one overhead light source and two smaller light sources in the background, one on each side of the scene. All object surfaces have measured reflectances applied to them: the floor is painted with gray primer, the flower pot shows the red clay reflectance, the squash shows the squash reflectance, the puzzle shows the red paint and the blue paint, and the hat is made out of black felt.

For reference, Figure 11 presents the same objects with only their diffuse reflectance components. Note how the illumination on the floor is mostly a result of the forward scattering of the light sources in the background. All of the surfaces exhibit scattering that varies with angle, which is especially visible along the silhouettes of the objects. While most effects could have been achieved by writing and carefully tweaking shaders for the rendering program, our measurement technique provides a more general and predictive approach to capture reflectance properties for rendering.

7 Conclusion

This paper has described a simple technique that can measure the BRDF of many materials using just a CCD camera and a light source. We achieve accuracy rivaling that of a specialized gonioreflectometer but with much greater speed and resolution, and with one twentieth the equipment cost. The technique is rapid because the two dimensions of a camera image sample two angular degrees of freedom instantaneously, leaving only one to be handled by sequential

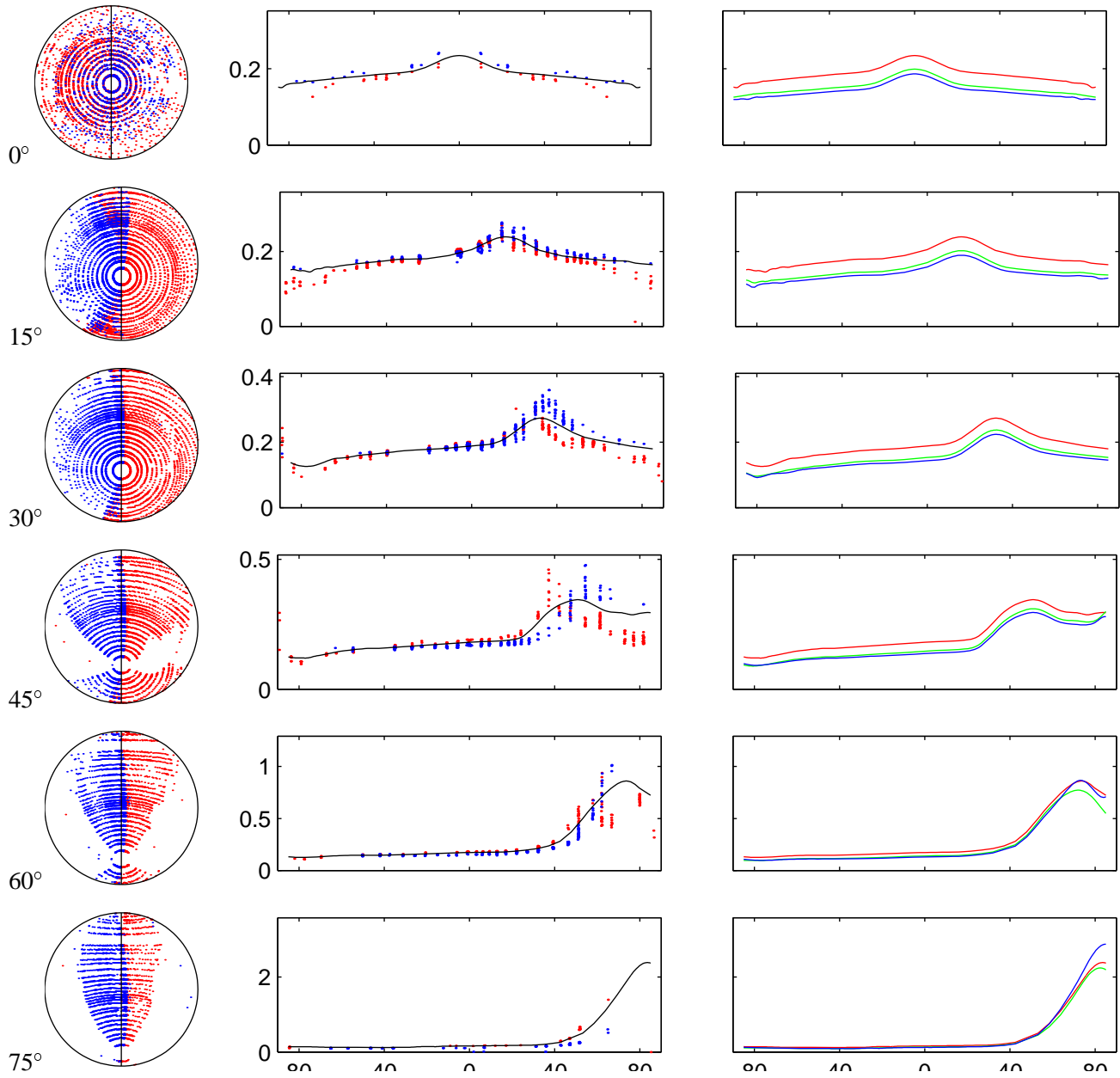


Figure 9: Summary of results for the squash dataset. Left column: sample coverage; middle column: incidence plane reciprocity and reconstruction; right column: incidence plane reconstruction for three color channels. Red points are fixed-incidence samples and blue are fixed-extant.

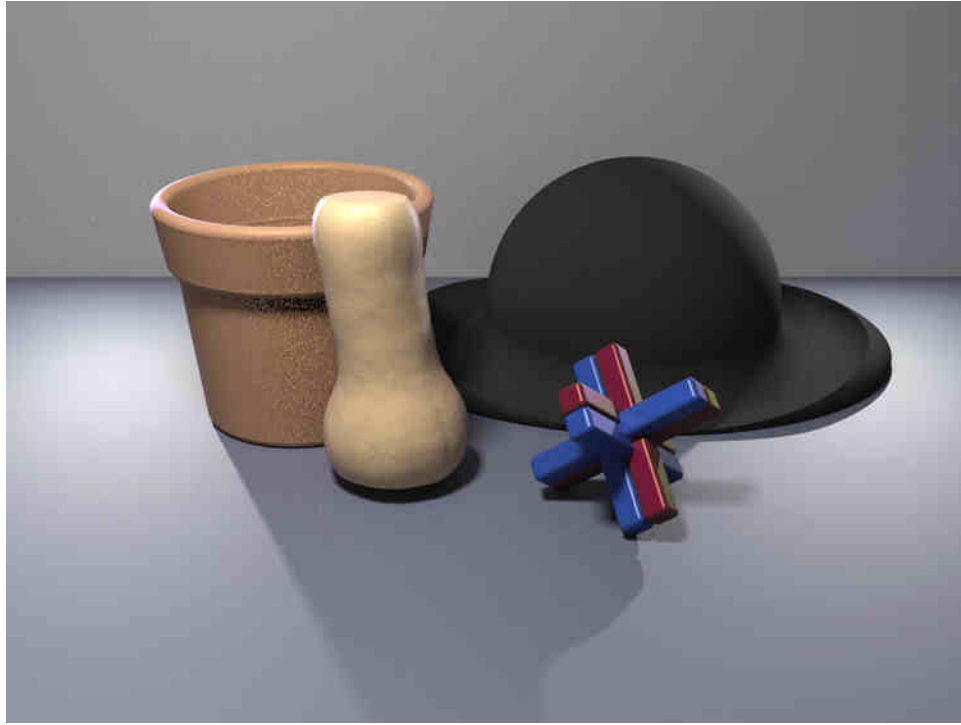


Figure 10: A rendered image showing a scene containing objects made of the measured materials.



Figure 11: A rendered image showing a scene containing diffuse objects with the same colors as the measured materials.

measurement. In a measurement session lasting under half an hour, our system can acquire millions of samples scattered over the full domain of an isotropic BRDF. The resulting data are internally consistent and agree closely with independent measurements.

Our technique is limited to measuring convex curved surfaces with uniform BRDFs. To measure the full hemispherical BRDF, a compound-curved surface is required, which may be found in the material's naturally occurring form or created by applying a man-made finish to a compound-curved surface. We can also measure the incidence-plane reflectance of a wider class of surfaces: any material that can be wrapped around a cylinder.

7.1 Future work

We have only demonstrated measurements of isotropic BRDFs. It should be possible to measure the BRDF of an anisotropic surface either by rotating the sample to provide a fourth degree of freedom or by moving the camera to positions over a quarter-sphere rather than a half-circle. This would require a test sample with uniform anisotropic BRDF and known orientation.

Our system could also be extended to allow non-convex surface shapes with the addition of shadow and visibility testing, along with a correction for global illumination. The ultimate system would be a combination scanner/reflectometer that produces a complete description of an object, including its full surface geometry and spatially varying BRDF across the entire surface.

BRDFs of very glossy surfaces have extremely high dynamic range, making them challenging to measure with any instrument. We applied a low-gloss finish to the colored paints to simplify this initial demonstration of the technique. We plan to extend our technique to glossier surfaces by making multiple exposures through different neutral density filters. As we measure glossier surfaces, we will have to take the finite source and detector solid angles into account.

References

- [1] Raymond J. Castonguay. New generation high-speed high-resolution hemispherical scatterometer. In John C. Stover, editor, *SPIE Proceedings*, volume 1995, pages 152–165, July 1993.
- [2] J. H. Chandler and C. J. Padfield. Automated digital photogrammetry on a shoestring. *Photogrammetric Record*, 15(88):545–559, 1996.
- [3] J. Fan and I. Gijbels. *Local Polynomial Modeling and Its Applications*. Chapman and Hall, London, 1996.
- [4] Sing-Choong Foo. A gonireflectometer for measuring the bidirectional reflectance of material for use in illumination computation. Master's thesis, Cornell University, 1997.
- [5] C. S. Fraser, M. R. Shortis, and G. Ganci. Multi-sensor system self-calibration. In *Videometrics IV*, pages 2–18. SPIE, oct 1995. Invited paper.
- [6] Andrew S. Glassner. *Principles of Digital Image Synthesis*. Morgan Kaufmann, San Francisco, 1995.
- [7] Anat Grynberg and Greg Ward. A new tool for reflectometry. Monograph 161, Lawrence Berkeley Laboratory, July 1990.
- [8] Ziad R. Hatab, John R. McNeil, and S. Sohail H. Naqvi. Sixteen-megabit dynamic random access memory trench depth characterization using two-dimensional diffraction analysis. *Journal of Vacuum Science and Technology B*, 13(2):174–181, March/April 1995.
- [9] Katsushi Ikeuchi and Kosuke Sato. Determining reflectance properties of an object using range and brightness image. *IEEE Transactions on Pattern Analysis and Machine Intelligence*, 13(11):1139–1153, 1991.

- [10] Konrad F. Karner, Heinz Mayer, and Michael Gervautz. An image based measurement system for anisotropic reflection. *Computer Graphics Forum (Eurographics '96 Proceedings)*, 15(3):119–128, August 1996.
- [11] Eric P. F. Lafortune, Sing-Choong Foo, Kenneth E. Torrance, and Donald P. Greenberg. Non-linear approximation of reflectance functions. In *Computer Graphics (SIGGRAPH '97 Proceedings)*, pages 117–126, August 1997.
- [12] Thomas A. Leonard and Michael Pantoliano. Brdf round robin. In *Stray Light and Contamination in Optical Systems*, 1988.
- [13] Rong Lu, Jan J. Koenderink, and Astrid M. L. Kappers. Optical properties (bidirectional reflectance distribution functions) of velvet. *Applied Optics*, 37(25):5974–5984, September 1998.
- [14] F. E. Nicodemus, J. C. Richmond, J. J. Hsia, I. W. Ginsberg, and T. Limperis. Geometric considerations and nomenclature for reflectance. Monograph 161, National Bureau of Standards (US), October 1977.
- [15] Yoichi Sato, Mark D. Wheeler, and Katsushi Ikeuchi. Object shape and reflectance modeling from observation. In *Computer Graphics (SIGGRAPH '97 Proceedings)*, pages 379–387, August 1997.
- [16] K. E. Torrance and E. M. Sparrow. Off-specular peaks in the directional distribution of reflected thermal radiation. In *Transactions of the ASME*, pages 1–8, Chicago, Ill., November 1965.
- [17] Gregory J. Ward. Measuring and modeling anisotropic reflection. In *Computer Graphics (SIGGRAPH '92 Proceedings)*, pages 265–272, July 1992.

A Additional Measurements

In addition to the gray cylinder and squash presented in detail in Section 6, we have measured several other materials. Using 200 mm diameter metal spheres as a substrate, we measured a blue latex enamel and a red metallic automotive lacquer; because both paints have high gloss finishes that exceed the dynamic range of our camera, we coated them with a lower-gloss finishing spray. The results for these paints are summarized in Figures 12 and 13. We located the spheres by fitting tangent spheres to grazing rays as described in Section 5.4, so there was no need to obscure any part of the surface with targets. This lack of occlusion, combined with the smooth shape of the spheres, leads to exceptionally uniform and complete domain coverage, as can be seen from the first column of each figure. The blue paint exhibits a classic diffuse plus specular behavior, as evidenced by the constant offset between the blue curve and the red and green. The red paint, on the other hand, has a much smaller diffuse component; its red color comes principally from a directional lobe that is higher and broader in the red than in the green and blue. This colored directional lobe is what gives the paint its metallic appearance.

An example of an object that gives less regular domain coverage is the clay flower pot, which is part cone and part cylinder (Figure 14). Since each component has curvature along only one direction, we expect the domain coverage to be concentrated near 2D surfaces rather than spread throughout the 3D domain. This lower-dimensional coverage is evident in the coverage plots, particularly at 15 and 30 degrees, where the points plainly cluster about curves.

The final example is a black felt hat (Figure 15). A black surface is a challenge for any reflectance measurement system, and while the data are noisier than the others they still reveal interesting features in the BRDF. The camera ADC quantization evident in the middle column is evidence of the extremely low signal levels involved; it is the very dense sampling of our method that lets us average to extract reasonable results from these data.

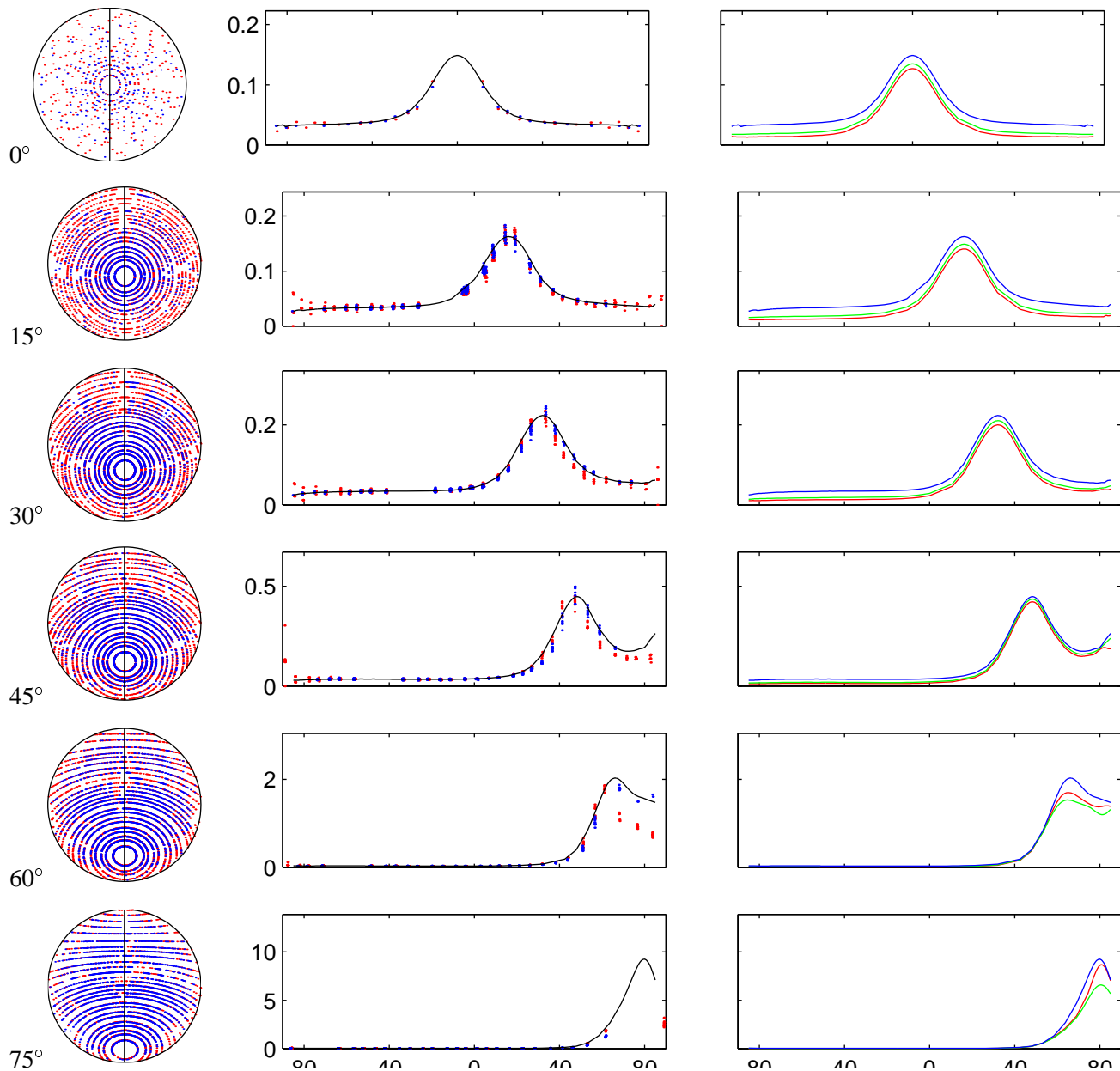


Figure 12: Summary of results for the blue sphere dataset. Left column: sample coverage; middle column: incidence plane reciprocity and reconstruction; right column: incidence plane reconstruction for three color channels. Red points are fixed-incidence samples and blue are fixed-extance.

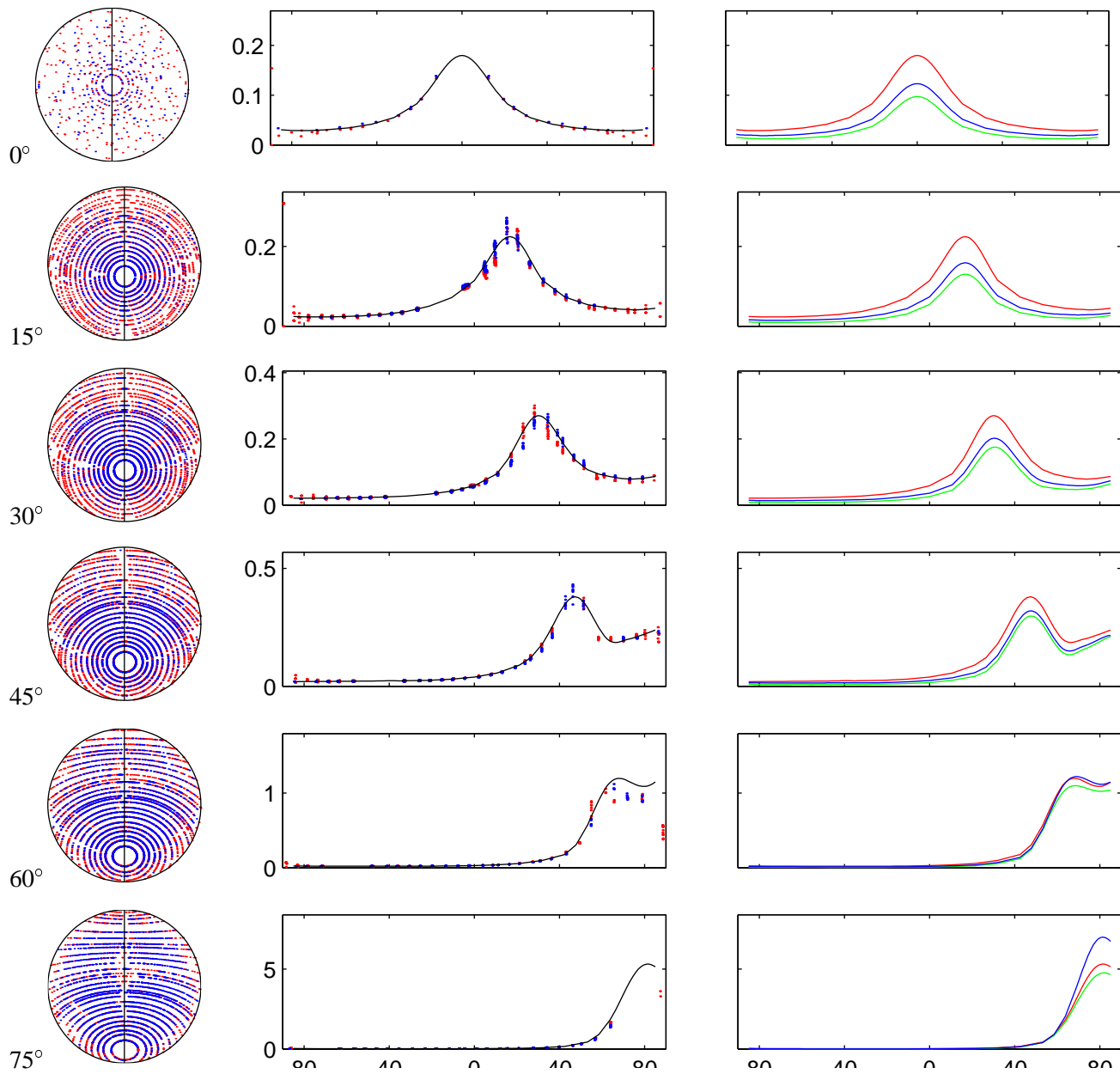


Figure 13: Summary of results for the red sphere dataset. Left column: sample coverage; middle column: incidence plane reciprocity and reconstruction; right column: incidence plane reconstruction for three color channels. Red points are fixed-incidence samples and blue are fixed-exitance.

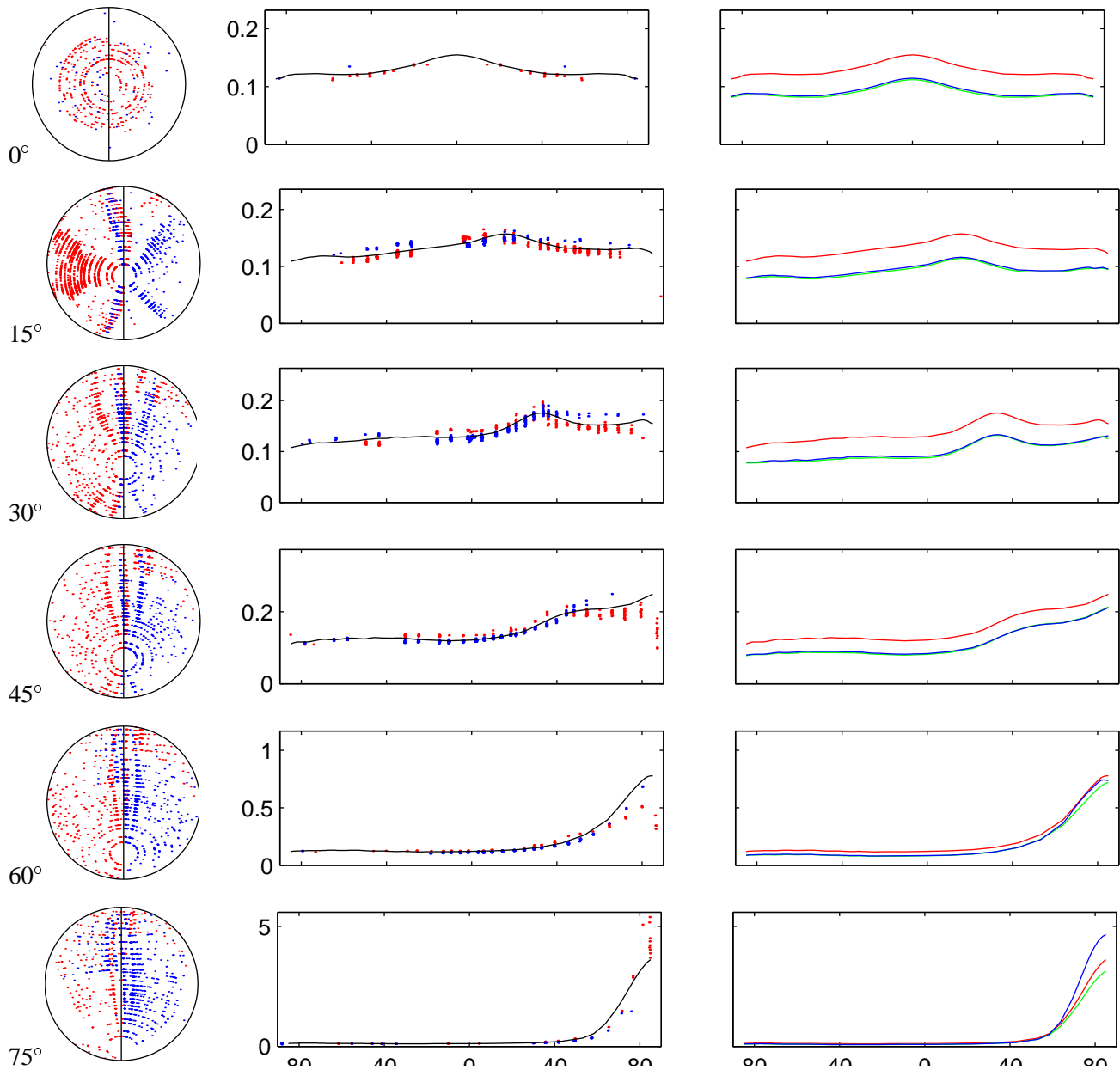


Figure 14: Summary of results for the clay pot dataset. Left column: sample coverage; middle column: incidence plane reciprocity and reconstruction; right column: incidence plane reconstruction for three color channels. Red points are fixed-incidence samples and blue are fixed-exitance.

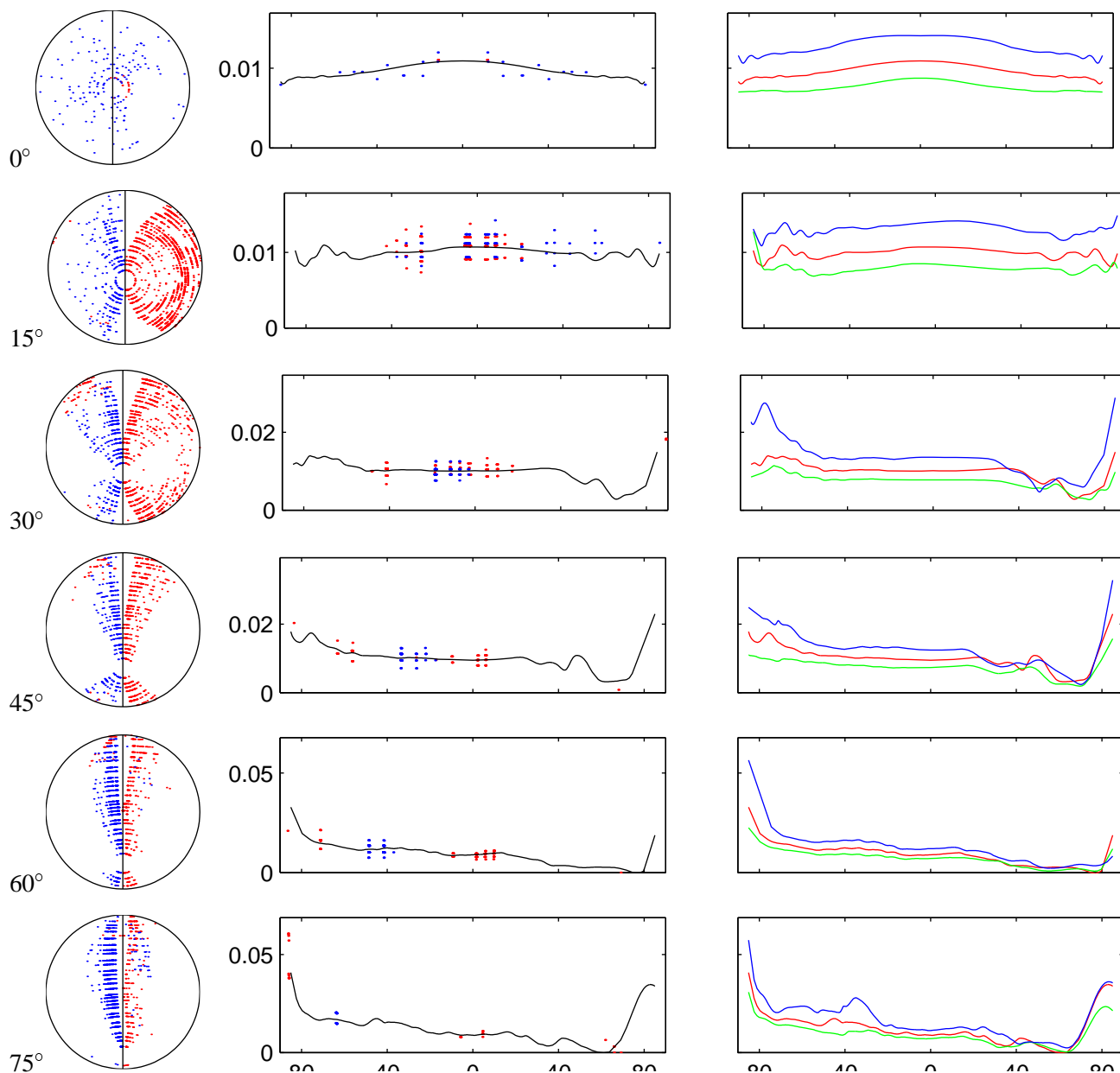


Figure 15: Summary of results for the felt hat dataset. Left column: sample coverage; middle column: incidence plane reciprocity and reconstruction; right column: incidence plane reconstruction for three color channels. Red points are fixed-incidence samples and blue are fixed-exitance.